Electronic Supplementary Material (ESI) for Physical Chemistry Chemical Physics.
This journal is © the Owner Societies 2022

Supporting Information: Hydration Dynamics and IR Spectroscopy of 4-Fluorophenol

Seyedeh Maryam Salehi, Silvan Käser, Kai Töpfer,[†] Polydefkis Diamantis,[‡] Peter Hamm,[¶] Ursula Röthlisberger,[‡] and Markus Meuwly[*,†]

†*Department of Chemistry, University of Basel, Klingelbergstrasse 80 , CH-4056 Basel, Switzerland.*

‡*Laboratory of Computational Chemistry and Biochemistry, Institute of Chemical Sciences and Engineering, École Polytechnique Fédérale de Lausanne, CH-1015 Lausanne, Switzerland.*

¶*Department of Chemistry, University of Zurich*

E-mail: m.meuwly@unibas.ch

Table S1: Molecular monopoles calculated using a fitting environment with GDMA algorithm for PhOH and F-PhOH.[1]

Atom (PhOH)	Charge (e)	Atom (F-PhOH)	charge (e)
C1	-0.095	C1	0.161
C2	-0.074	C2	-0.060
C3	-0.079	C3	-0.061
C4	0.075	C4	0.064
C5	-0.079	C5	-0.061
C6	-0.074	C6	-0.060
H7	0.086	H7	0.113
H8	0.102	H8	0.105
H9	0.102	H9	0.105
H10	0.086	H10	0.113
O11	-0.392	O11	-0.389
H12	0.259	H12	0.260
H13	0.082	F13	-0.291

Table S2: Atomic dipoles for PhOH and F-PhOH from fitting to the molecular electrostatic potential.[1] Qxx are the spherical MTP coefficients expressed in the local axis system.

Atom	Q10 (e)	Q11c (e)	Q11s (e)
PhOH			
C1	-0.015	0.0	0.033
C2	-0.016	-	0.030
C3	-0.0002	-	0.054
C4	0.028	0.0	0.089
C5	-0.0002	-	0.054
C6	-0.016	-	0.030
O11	0.0	0.099	-0.070
H13	0.0	0.0	0.0
F-PhOH			
C1	-0.011	0.0	0.180
C2	-0.022	-	0.073
C3	-0.025	-	0.017
C4	0.015	0.0	0.122
C5	-0.025	-	0.017
C6	-0.022	-	0.073
O11	0.0	0.121	-0.140
F13	0.147	0.0	0.008

Table S3: Atomic quadrupoles for PhOH and F-PhOH from fitting to the molecular electrostatic potential.[1] Qxx are the spherical MTP coefficients expressed in the local axis system.

Atom	Q20 (e)	Q21c (e)	Q21s (e)	Q22c(e)	Q22s(e)
PhOH					
C1	-0.029	0.0	0.001	-0.005	0.0
C2	-0.026	-	-0.0003	-0.0013	-
C3	-0.012	-	0.002	0.0039	-
C4	8.04×10^{-5}	0.0	0.013	0.0015	0.0
C5	-0.012	-	0.0029	0.0039	-
C6	-0.0260	-	-0.0003	-0.0013	-
O11	-0.006	0.0	0.0	0.015	-0.0278
H13	0.0	0.0	0.0	0.0	0.0
F-PhOH					
C1	-0.024	0.0	0.006	-0.007	0.0
C2	-0.042	-	0.003	0.0005	-
C3	-0.029	-	0.002	0.009	-
C4	0.005	0.0	0.022	-0.009	0.0
C5	-0.029	-	0.002	0.009	-
C6	-0.042	-	0.003	0.0005	-
O11	-0.034	0.0	0.0	0.029	-0.0798
F13	-0.034	0.0	0.0016	0.009	0.0

Table S4: The frequency maxima obtained from frequency distribution, power and IR spectrum using PC/MTP model in the gas phase and solvent for five different modes in the frequency range of 1100 to 1400 cm^{-1} .

MD								
Mode	$P(\omega)$		PS(CF)		PS(CF)		IR(CF)	
	MTP_{gas}	MTP_{H_2O}	MTP_{gas}	MTP_{H_2O}	PC_{gas}	PC_{H_2O}	PC_{H_2O}	MTP_{H_2O}
ν_1	1140	1149	1141	1158	1140	1163	1148	1151
ν_2	1170	1172	1170	1185	1171	1184	1172	1174
ν_3	1225	1236/1251	1227	1248	1226	1265	1243	1249
ν_4	1286	1294	1285	1305	1286	1310	1294	1296
ν_5	1324	1330	1324	1345	1324	1343	1331	1333

Table S5: Parameters obtained from fitting the FFCF to Eq. 3 based on frequencies from INM using 5 ns MTP (10^6 snapshots) simulation of F-PhOH in H_2O. Average frequency $\langle\omega\rangle$ of the asymmetric stretch in cm^{-1}, the amplitudes a_1 and a_2 in ps^{-2}, the decay times τ_1 and τ_2 in ps, and the offset Δ_0 in ps^{-2}. The FFCF for the OH-stretch is reported in Figure S12.

Mode	$\langle\omega\rangle$	a_1	τ_1	a_2	τ_2	Δ_0
ν_1	1149.71	0.36	0.08	0.06	0.45	0.0005
ν_2	1173.00	0.29	0.05	0.04	0.38	0.0003
ν_3	1248.40	2.31	0.10	0.32	0.60	0.0095
ν_4	1295.18	0.68	0.08	0.14	0.28	0.0029
ν_5	1332.04	1.01	0.09	0.06	0.83	0.0055
OH	3500.22	32.11	0.10	17.72	0.50	0.19

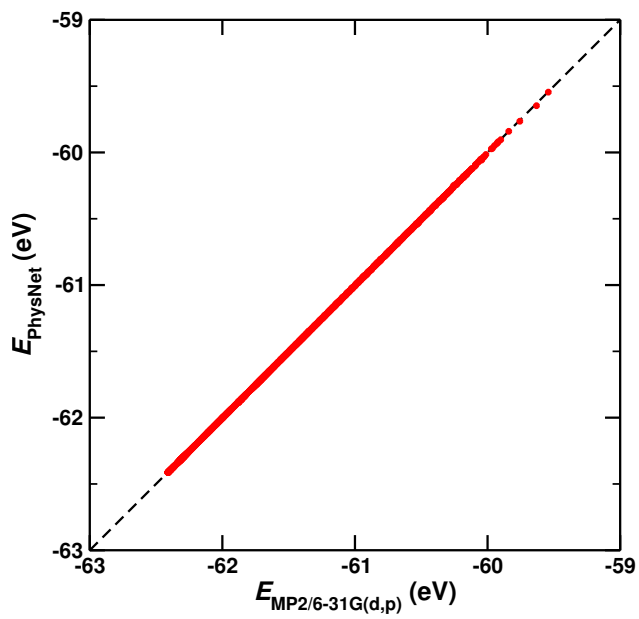

Figure S1: Correlation between the ab initio and PhysNet energies for a set of 3700 randomly selected points averaged over 980/982 trajectories with $R^2 = 0.9999$ and an root mean square error of 0.0037 eV.

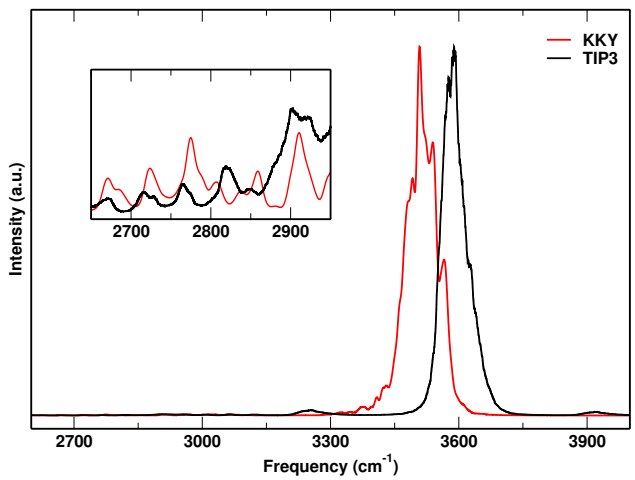

Figure S2: The power spectrum for the phenol-OH stretching vibration from a 5 ns simulation of F-PhOH with flexible (red) KKY water[2–4] compared to TIP3 (black) model. The red shift from the simulations with KKY is –78 cm^{-1}.

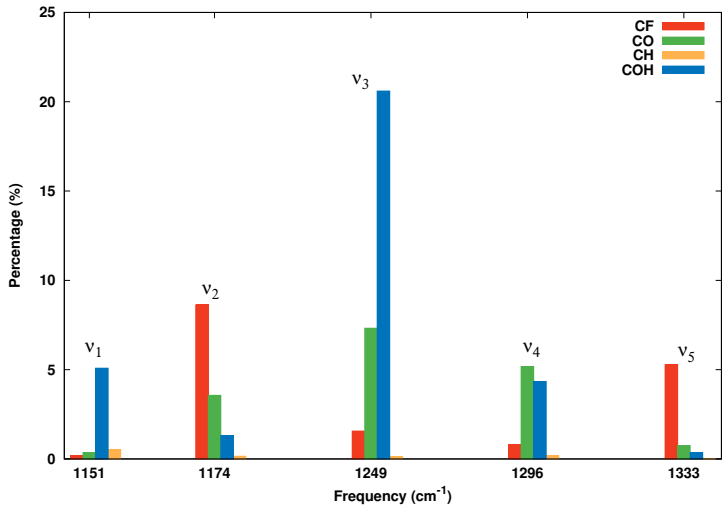

Figure S3: Participation ratio of the CF (red), CO (green), and CH (orange) stretching and the COH bending (blue) motions to the 5 modes between 1140 and 1350 cm^{-1} by using the "project" facility in CHARMM for 10^5 snapshots from the MTP simulation of F-PhOH in H_2O. The remaining contributions are from low frequency modes.

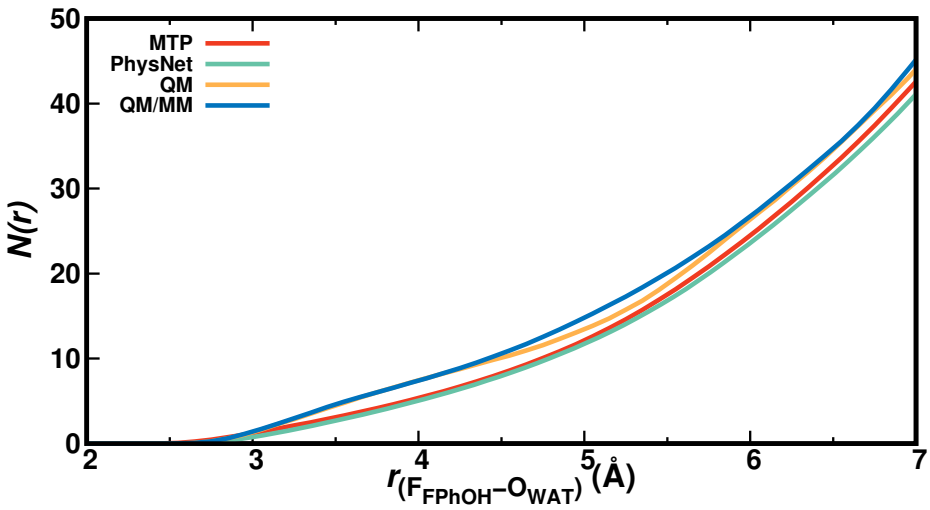

Figure S4: The total number of water molecules within distance r of the fluorine atom for the MTP (red), PhysNet (green), QM/MM (orange) and QM (blue) simulations.

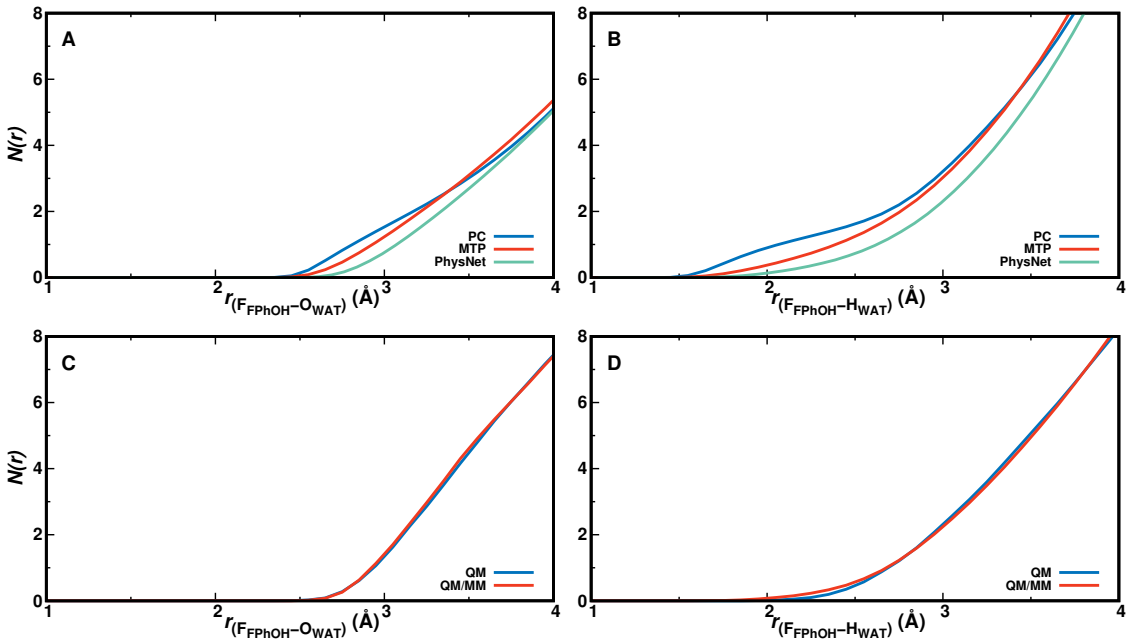

Figure S5: The $N(r)$ for F-O_{WAT} (panel A) and F-H_{WAT} (panel B) separations from PC (blue), MTP (red) and PhysNet (green) simulations of F-PhOH in H_2O. Panels C and D show the results from QM (blue) and QM/MM (red) simulations.

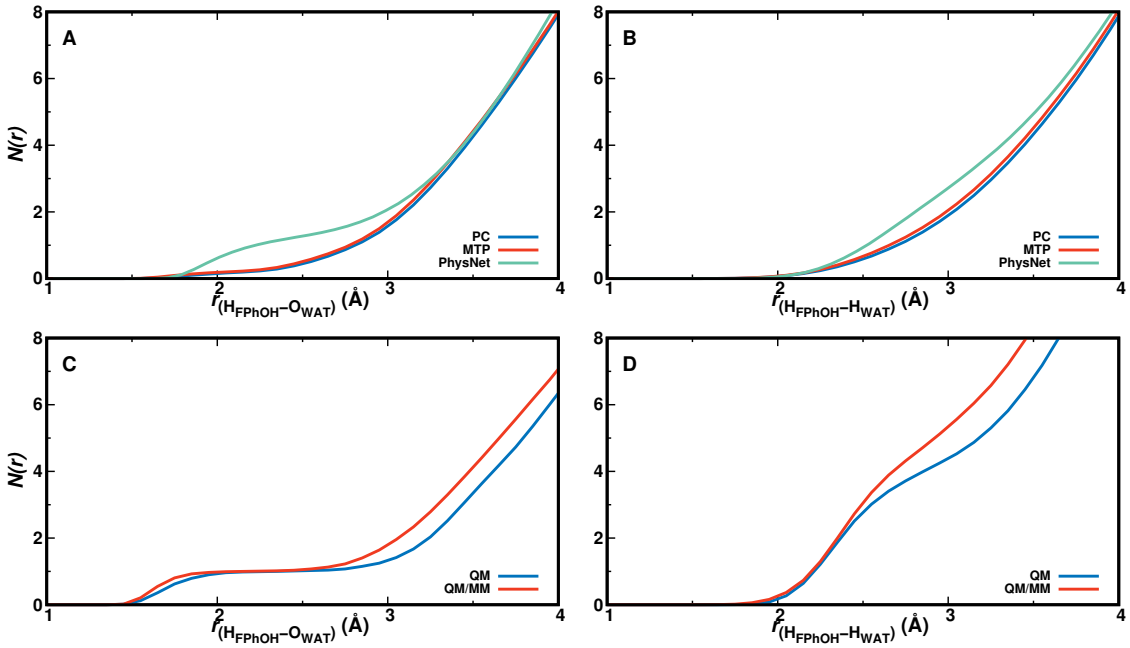

Figure S6: The $N(r)$ for $H_{FPhOH/PhOH}$-O_{WAT} (panel A) and $H_{FPhOH/PhOH}$-H_{WAT} (panel B) distances between the H-atom of the solute OH-group as obtained from PC (blue), MTP (red) and PhysNet (green) simulations for F-PhOH in H_2O. Panels C and D for results from QM (blue) and QM/MM (red) simulations.

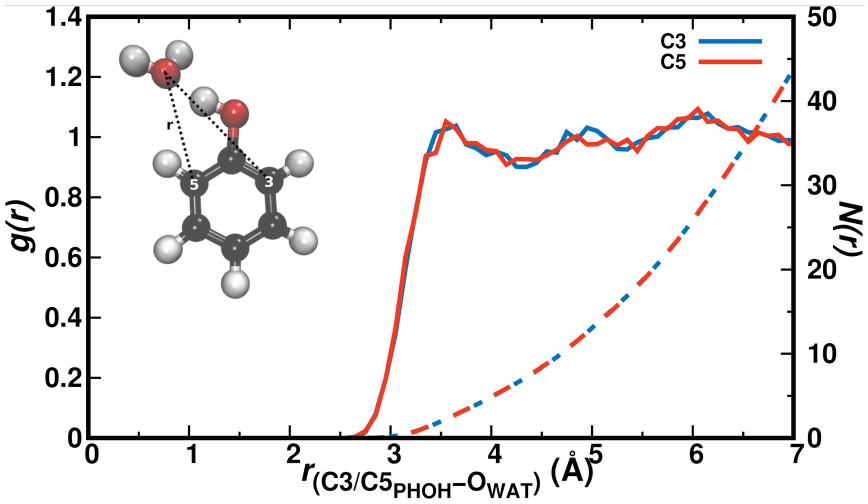

Figure S7: The radial distribution function between the water-oxygen atoms and the two carbon atoms flanking the COH group in PhOH from a 5 ns simulation with MTP. It is demonstrated that the solvent distribution is converged. Comparison with the red trace in Figure 4A indicates that hydration around the CF and CH groups is similar with the first maximum at a similar C–O_W separation.

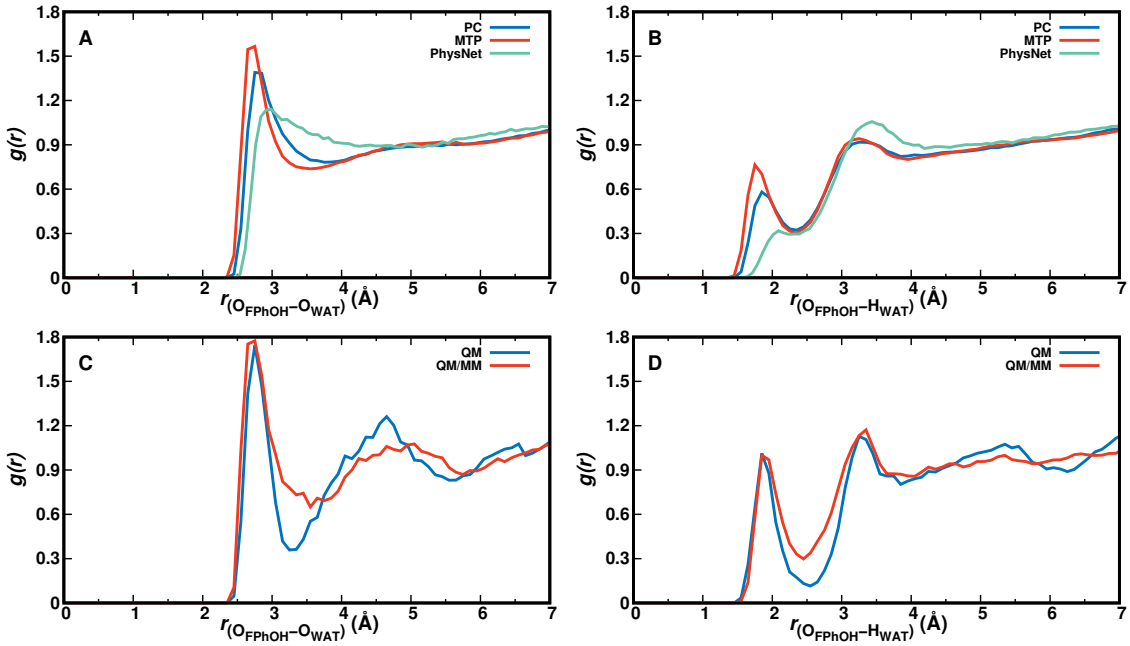

Figure S8: The $g(r)$ for A) O_{FPhOH}-O_{WAT} and B) O_{FPhOH}-H_{WAT} distances as obtained from PC (blue), MTP (red) and PhysNet (green) simulations of F-PhOH in H_2O. Panel C and D from QM and QM/MM simulations.

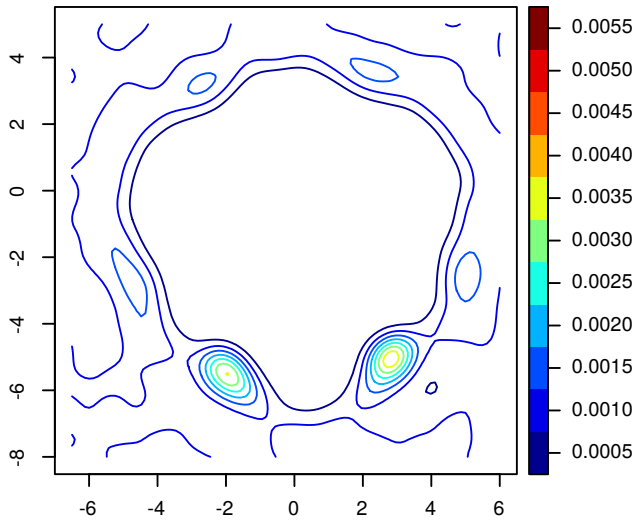

Figure S9: 2d-distribution from MTP simulations with TIP3P water. The structures are re-oriented with reference to the solute heavy atoms, but excluding the phenolic-oxygen atom. This differs from the selection used in Figure 6 and allows to visualize the symmetric distribution of the solvent water molecules around the -COH group.

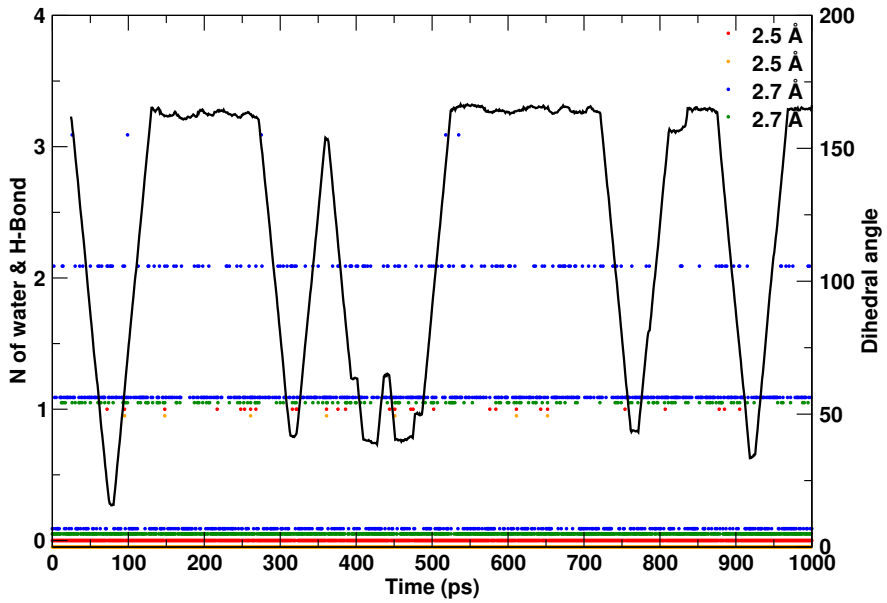

Figure S10: Dihedral rotation of the CCOH angle together with the water occupation of the -OH group (circles) and number of H-bonds (crosses) for O_{COH}–O_W separations of a) 2.5 Å (red & orange) and b) 2.7 Å (blue & green). With the shorter cutoff there is no water molecule hydrogen bonded to the rotatable COH group for most of the simulation time and occasionally one water is sufficiently close to form an H-bond. For the longer cutoff water presence is frequent and H-bounding (green crosses) is more prevalent. The alteration between H-bonded and non-H-bonded -COH group explains the spectroscopy seen in Figure S2. A direct correlation between rotation of the CCOH angle and water occupation can not be established convincingly although it is likely that rotation of the COH group requires water to detach from it. The dihedral time series is locally averaged over a time window of 50 ps. Simulations with ML/MM MD yield a comparable time series with transitions on the $\sim$ 100 ps time scale..

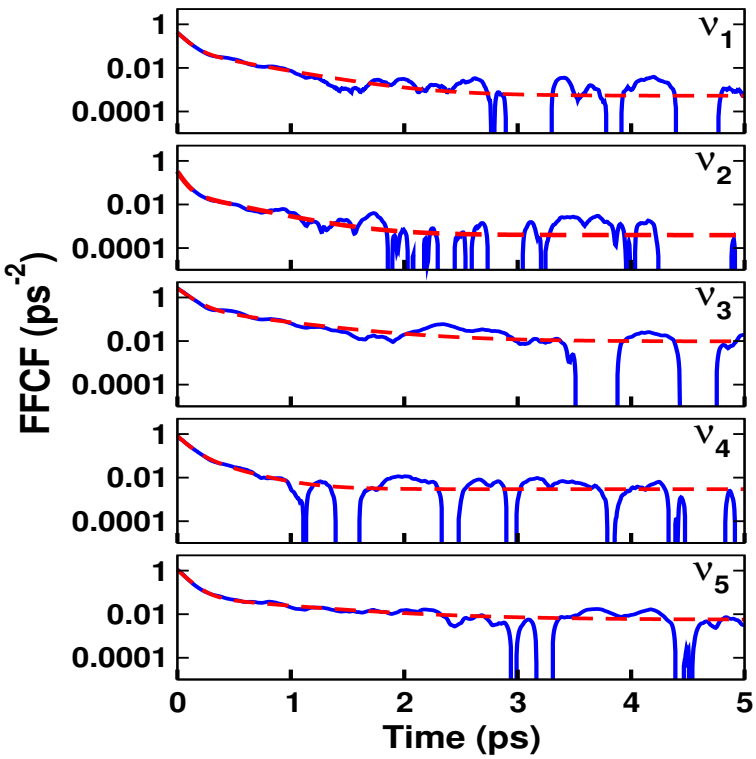

Figure S11: FFCFs from INM frequency calculations for F-PhOH in water from a 5 ns simulation using MTP. The FFCFs for the 5 modes ν_1 to ν_5 between 1100 and 1400 cm^{-1} are reported. The solid lines are the raw FFCF data and the dashed lines show the corresponding fit with fitting parameters reported in Table S5. Logarithmic scale is chosen for the y-axis.

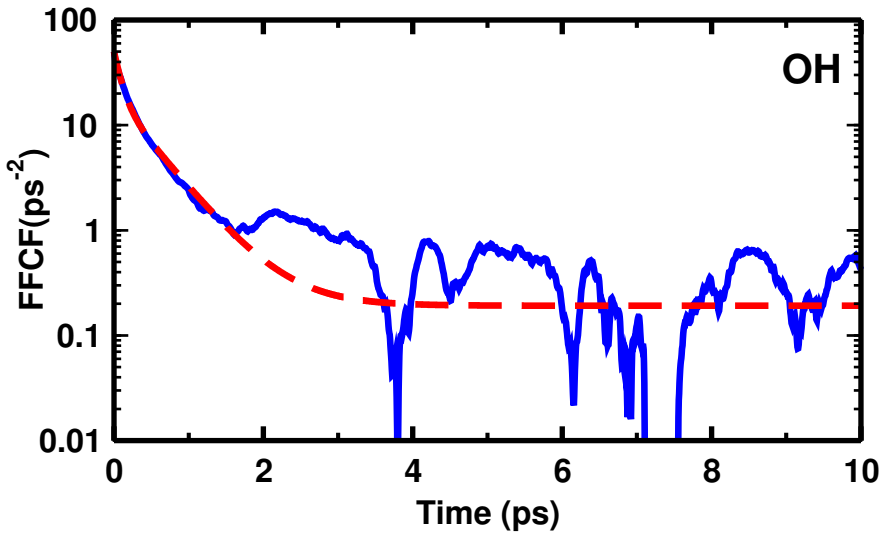

Figure S12: FFCFs from INM frequency calculations for F-PhOH in water from a 5 ns simulation using MTP. The FFCFs for the OH mode is reported. The solid lines are the raw FFCF data and the dashed lines show the corresponding fit with fitting parameters reported in Table 2. Logarithmic scale is chosen for the y-axis.

References

(1) Hedin, F.; El Hage, K.; Meuwly, M. A Toolkit to Fit Nonbonded Parameters from and for Condensed Phase Simulations. *J. Chem. Theo. Comp.* **2016**, *56*, 1479–1489.

(2) Burnham, C. J.; Li, J. C.; Leslie, M. Molecular Dynamics Calculations for Ice Ih. *J. Phys. Chem. B* **1997**, *101*, 6192–6195.

(3) Plattner, N.; Meuwly, M. Atomistic Simulations of CO Vibrations in Ices Relevant to Astrochemistry. *ChemPhysChem* **2008**, *9*, 1271–1277.

(4) Kumagai, N.; Kawamura, K.; Yokokawa, T. An Interatomic Potential Model for H_2O: Applications to Water and Ice Polymorphs. *Mol. Sim.* **1994**, *12*, 177–186.